Purcell effect of GaAs quantum dots by photonic crystal microcavities

Kazuaki Sakoda[1,3*], Takashi Kuroda[1], Naoki Ikeda[1], Takaaki Mano[1], Yoshimasa Sugimoto[1], Tetsuyuki Ochiai[1], Keiji Kuroda[1], Shunsuke Ohkouchi[2], Nobuyuki Koguchi[1], and Kiyoshi Asakawa[1]

[1] *National Institute for Materials Science, 1-2-1 Sengen, Tsukuba 305-0047, Japan*

[2] *NEC Corporation, 34 Miyukigaoka, Tsukuba 305-8501, Japan*

[3] *Graduate School of Pure and Applied Sciences, University of Tsukuba, 1-1-1 Tennodai, Tsukuba 305-8577, Japan*

[*] *E-mail: sakoda.kazuaki@nims.go.jp*

Received July 14, 2009

We fabricate photonic crystal slab microcavities embedded with GaAs quantum dots by electron beam lithography and droplet epitaxy. The Purcell effect of exciton emission of the quantum dots is confirmed by the micro photoluminescence measurement. The resonance wavelengths, widths, and polarization are consistent with numerical simulation results.

OCIS codes: 050.5298, 230.5590, 300.2140.
doi: 10.3788/COL20090710.0879.

The development of high-performance microcavities in photonic crystal (PC) slabs[1,2] has enabled us to investigate the cavity quantum electrodynamics (QED) with light-emitting semiconductor nanostructures embedded in them[3−9]. Yoshie *et al.*[3] reported the Purcell effect[10] and the vacuum Rabi splitting of InAs quantum dots (QDs) embedded in a PC slab with a microcavity. Englund *et al.*[4] reported both acceleration and suppression of photoluminescence (PL) of InAs QDs in the cavity resonance and off-resonance cases, respectively. Badolato *et al.*[5] and Hennessy *et al.*[6] observed the Purcell effect and the vacuum Rabi splitting of position-controlled InAs QDs by tuning the cavity resonance frequency by their digital etching technique, respectively. Kress *et al.*[7] and Chang *et al.*[8] observed the Purcell effect of InGaAs QDs. For further cavity QED experiments, QDs with emission lines of shorter wavelengths are desirable, since silicon photodetectors with high quantum efficiencies are applicable. We recently reported the Purcell effect of GaAs QDs with emission wavelengths around 750 nm[9], which lie in the desirable wavelength range.

In this letter, we report the polarization dependence of the Purcell effect of GaAs QDs embedded in PC slabs with various lattice constants, which is brought about by two cavity modes with different frequencies and polarizations. We also show the spectral narrowing of emission lines in the case of weak continuous-wave (CW) photo excitation and discuss its possible origin.

Specimens for the present experiments were fabricated as described in Ref. [9]. In brief, GaAs QDs were fabricated on an AlGaAs layer by the droplet epitaxy[11,12]. Then a triangular array of cylindrical air holes was made by the electron beam lithography and successive etching. A sacrificial under-layer was removed by wet etching to form an air-bridged PC slab. Figure 1 shows a scanning electron microscope (SEM) image of one of our specimens. The distance between centers of adjacent air holes (lattice constant) is about 200 nm and their radius is about 60 nm. In the center of the specimen, three holes are missing. This structure is called L3 cavity and is known to give high-quality-factor (high-Q) microcavities[1]. Although the Q factor of the cavity may be increased by introducing appropriate shifts of air-hole positions[1,2], we did not introduce them, since microcavities with Q factors around 1000 were sufficient for our experiments by the reason that we will describe later.

As for GaAs nanostructures on the AlGaAs barrier layer, we have established their fabrication method, and specimens of various shapes can be made, as shown in Fig. 2. The fabrication condition was chosen to obtain well-defined QDs with an area density of 50 μm^{-2}.

Micro PL spectra of the specimens were measured by a home-made confocal microscope. The excitation light source was provided by the second harmonic of the output of an optical parametric oscillator (OPO) excited by a femtosecond Ti: sapphire laser and a CW helium laser. The micro PL spectra were detected by a single-grating monochromator with a charge-coupled device (CCD) detector. All measurements were done at liquid helium temperature. The simulation of the cavity mode was done with a home-made software by the finite-difference time-domain (FDTD) method with the perfectly-matched absorbing

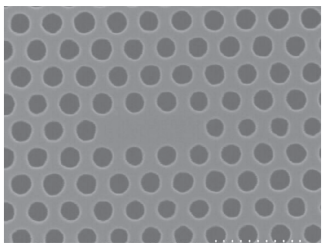

Fig. 1. SEM image of a photonic crystal slab with an L3 defect cavity.

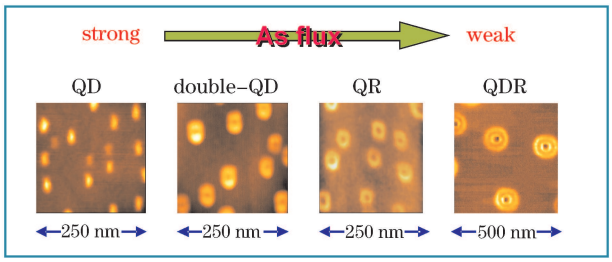

Fig. 2. Various nanostructures that can be fabricated by droplet epitaxy. QR: quantum ring; QDR: quantum double-ring.

Table 1. Characteristics of Four Modes of the L3 Cavity

Parity	Polarization	Wavelength (nm)	Q
(e, e, e)		706	355
(e, o, e)	y	763	5600
(o, e, e)	x	711	402
(o, o, e)		711	533

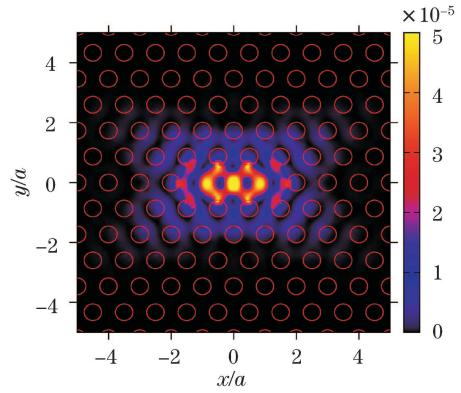

Fig. 3. Distribution of the electric field of the (e, o, e) symmetry cavity mode calculated by the FDTD method. a is the lattice constant.

boundary condition[13].

By the FDTD simulation, we found four cavity modes of the L3 cavity, which are listed in Table 1. In the calculation, we assume that the lattice constant is 207 nm, the thickness of the PC slab is 120 nm, and the radius of the air holes is 57.5 nm. The cavity modes are characterized by their particular polarization properties. To describe them, we take the x and y axes along the long and short axes of the L3 cavity, and take the z axis perpendicular to the sample surface. Then the structure of the L3 cavity has the mirror symmetry for the yz, zx, and xy planes. So, the electromagnetic eigenmodes of the cavity must have even (e) or odd (o) parity about these mirror planes.

Among the four cavity modes listed in Table 1, only two modes with (e, o, e) and (o, e, e) parities are compatible with the symmetry of plane waves propagating perpendicular to the surface of the specimen. The former couples to a y-polarized plane wave, whereas the latter couples to an x-polarized plane wave. Their Q factors are quite different from each other. The former has a Q factor as high as 5600 if the imaginary part of the dielectric constant of the specimen is negligible.

Figure 3 shows the distribution of the electric field intensity of the (e, o, e) mode. It has several nodes of the electric field amplitude. So, if the position of the QD happens to coincide with one of the nodes, then the coupling strength between its electronic system and the cavity mode is exactly equal to zero. On the contrary, if the position coincides with the field maximum, then the coupling becomes large to result in the acceleration of spontaneous emission of photons, which is known as the Purcell effect. In our experiment, the QDs were fabricated by self-assembly so that their positions in the cavity were random. In addition, their exciton emission wavelengths depended on their size due to the quantum-confinement effect so that they also had a random distribution. To match the emission wavelengths to the cavity resonance wavelengths, we designed cavities with relatively small Q factors to widen the full-width at half-maximum (FWHM) of the resonance.

In Ref. [9], we reported the acceleration by the Purcell effect and the suppression by the photonic band gap of the spontaneous emission of photons. We also showed the change in the cavity resonance wavelength due to the change in the lattice constant of the specimen. However, we focused on the emission through the (e, o, e) mode by the pulsed excitation, since we were mainly interested in the lifetime of the PL influenced by the presence of the PC cavity. On the other hand, we will describe the emission through the (o, e, e) mode and the case of the CW excitation in more detail in the following to give further evidence for the Purcell effect.

Figure 4 shows the micro PL spectra of both x and y polarizations for specimens with lattice constants of 206 and 209 nm. For the former specimen, the resonance wavelength of the (o, e, e) mode is out of the emission range of the GaAs QDs so that only one resonance peak for the y polarization is observed. On the other hand, the resonance wavelength is larger for the latter specimen and both peaks are observed. As shown in Table 1, the Q factor of the (o, e, e) mode is smaller than that of the (e, o, e) mode by about one order of magnitude, the FWHM of the resonance curve of the former is large, and we can see that several exciton emission lines are located in the resonance and enhanced.

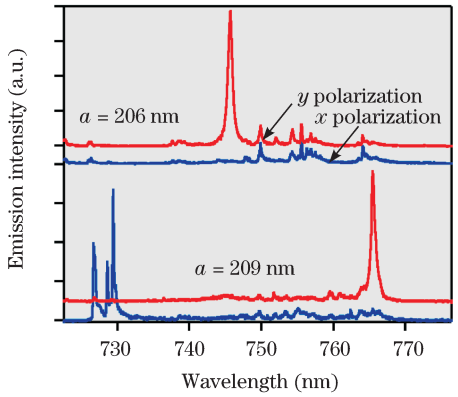

Fig. 4. Polarization dependence of the micro PL spectra from GaAs QDs embedded in L3 cavities with lattice constants of 206 and 209 nm. The excitation light source with a wavelength of 660 nm is provided by a femtosecond laser system.

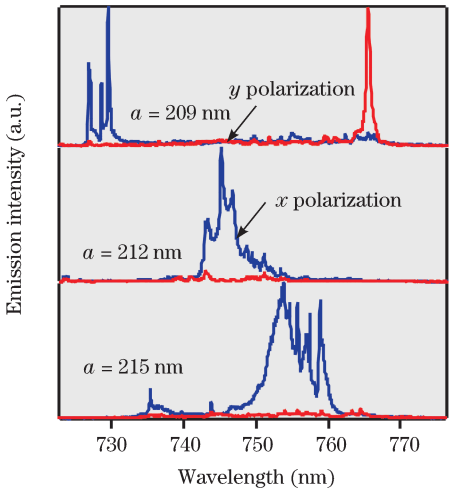

Fig. 5. Micro PL spectra for specimens with three different lattice constants for both x and y polarizations measured with a femtosecond excitation light source.

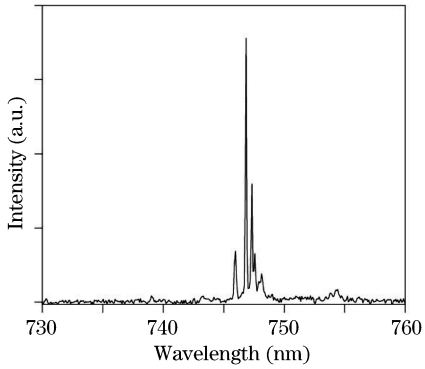

Fig. 6. Micro PL spectrum with the y polarization measured for the same specimen as Fig. 4 with a CW excitation light source.

This feature can be found more clearly in Fig. 5, where emission spectra of the x and y polarizations are compared among specimens with lattice constants of 209, 212, and 215 nm. For the latter two specimens, the resonance wavelength of the (e, o, e) mode is out of the exciton emission range and no peak is observed for the y polarization. On the other hand, there are enhanced emission bands for the x polarization, which consist of several narrower emission lines. The shapes of the emission bands naturally have a random feature originating from the random distribution of positions and the emission wavelength of the self-assembled QDs.

So far, we used a pulsed laser system for the excitation light source because we used the same light source for the emission lifetime measurement in our previous research[9]. However, the widths of the exciton emission lines are broadened by the multi-carrier effect under the pulsed excitation by a femtosecond laser. Actually, each emission line becomes narrower when we excite the specimen with a weak CW laser beam, as shown in Fig. 6. Here the specimen is the same as that in Fig. 4 with a lattice constant of 206 nm and only the spectrum for the y polarization is shown. We can see that the broad resonance peak in the upper panel of Fig. 4 is composed of several exciton emission lines.

In conclusion, we fabricated many PC slab microcavities with different lattice constants with embedded GaAs QDs and carefully observed micro PL spectra of the exciton emission. We found the polarization dependent peaks in the spectra and attributed them to the enhancement due to the Purcell effect. Their resonance wavelengths and widths were consistent with the results of the FDTD simulation. Under the pulsed excitation by a femtosecond laser system, the resonance peaks were broadened by the multi-carrier effect. When a weak CW laser was used for the excitation, we could observe the genuinely narrow but enhanced emission lines of excitons whose linewidths were apparatus-limited.

This work was supported by a Grant-in-Aid for Scientific Research from the Ministry of Education, Science, Sports, and Culture of Japan under Grant No. 20340080.

References

1. Y. Akahane, T. Asano, B.-S. Song, and S. Noda, Nature **425,** 944 (2003).
2. Y. Akahane, T. Asano, B.-S. Song, and S. Noda, Opt. Express **13,** 1202 (2005).
3. T. Yoshie, A. Scherer, J. Hendrickson, G. Khitrova, H. M. Gibbs, G. Rupper, C. Ell, O. B. Shchekin, and D. G. Deppe, Nature **432,** 200 (2004).
4. D. Englund, D. Fattal, E. Waks, G. Solomon, B. Zhang, T. Nakaoka, Y. Arakawa, Y. Yamamoto, and J. Vučković, Phys. Rev. Lett. **95,** 013904 (2005).
5. A. Badolato, K. Hennessy, M. Atatüre, J. Dreiser, E. Hu, P. M. Petroff, and A. Imamoğlu, Science **308,** 1158 (2005).
6. K. Hennessy, A. Badolato, M. Winger, D. Gerace, M. Atatüre, S. Gulde, S. Fält, E. L. Hu, and A. Imamoğlu, Nature **445,** 896 (2007).
7. A. Kress, F. Hofbauer, N. Reinelt, M. Kaniber, H. J. Krenner, R. Meyer, G. Böhm, and J. J. Finley, Phys. Rev. B **71,** 241304 (2005).
8. W.-H. Chang, W.-Y. Chen, H.-S. Chang, T.-P. Hsieh, J.-I. Chyi, and T.-M. Hsu, Phys. Rev. Lett. **96,** 117401 (2006).
9. T. Kuroda, N. Ikeda, T. Mano, Y. Sugimoto, T. Ochiai, K. Kuroda, S. Ohkouchi, N. Koguchi, K. Sakoda, and K. Asakawa, Appl. Phys. Lett. **93,** 111103 (2008).
10. E. M. Purcell, Phys. Rev. **69,** 681 (1946).
11. N. Koguchi, S. Takahashi, and T. Chikyow, J. Cryst. Growth **111,** 688 (1991).
12. T. Mano, T. Kuroda, K. Kuroda, and K. Sakoda, J. Nanophoton. **3,** 031605 (2009).
13. A. Taflove, *Computational Electrodynamics: Finite Difference Time Domain Method* (Artech House, Boston, 1995).